Stochastic Thermal Diffusion Forced Rayleigh Scattering[1]

R. Schäfer[2], A. Becker[2], and W. Köhler[2,3]

[1] Paper presented at the Thirteenth Symposium on Thermophysical Properties, June 22-27, 1997, Boulder, Colorado, U.S.A.

[2] Max-Planck-Institut für Polymerforschung, Postfach 3148, D-55021 Mainz, Germany.

[3] To whom correspondence should be addressed.

Abstract

The holographic grating technique of thermal diffusion forced Rayleigh scattering (TDFRS) utilizes the Ludwig-Soret effect to induce a concentration modulation within a binary liquid. The signal generation is described in terms of a linear response formalism, and the memory function for the concentration mode $g(t)$ and its Fourier transformed, the diffusion susceptibility, are measured by means of pseudostochastic random binary sequences with flat power spectra in combination with fast Fourier transform and correlation techniques. For polydisperse polymer solutions the individual modes contribute proportional to their concentration to $g(t)$, contrary to photon correlation spectroscopy, where the correlation function is dominated by the high molar mass components. Other advantages of stochastic TDFRS are time scale delocalization of dust spikes and frequency multiplexing. Measurements are reported on monodisperse and bimodal polystyrene in toluene.

KEY WORDS: diffusion, forced Rayleigh scattering, Fourier transform, Ludwig-Soret effect, polymer solutions, stochastic excitation, thermal diffusion

1 Introduction

A holographic interference grating written into a binary liquid, e.g. a polymer solution, gives rise to a secondary concentration grating driven by the Ludwig-Soret effect, also termed thermal diffusion [1, 2, 3]. From such thermal diffusion forced Rayleigh scattering (TDFRS) experiments various transport coefficients, like the thermal diffusivity, the mutual diffusion coefficient, the thermal diffusion coefficient, and the Soret coefficient, can be determined in a very direct way. Due to the μm diffusion length, the corresponding subsecond diffusion times, and the very subtle perturbations of the sample, many problems associated with long term stability in traditional diffusion cell experiments disappear.

With respect to the measurement of center of mass diffusion there exist several similarities between TDFRS and photon correlation spectroscopy (PCS), but also significant differences. PCS relies on thermodynamic concentration fluctuations. In dilute polymer solutions the scattering, which is proportional to the molar mass, is dominated by the high molar mass components, and few heavy particles, can completely mask low molar mass contributions.

TDFRS, on the other hand, allows for a coherent excitation with a single well defined q-vector. Since thermal diffusion is driven by the applied temperature grating, there is considerable freedom in the selection of the excitation time pattern, and periodic amplitude modulation has been proposed in the literature [4].

It has been shown that for dilute polymer solutions TDFRS can be employed for polydispersity analysis of dilute polymer solutions. The memory or the linear response function, which fully characterizes a linear system, is of particular interest because of the even concentration proportional statistical weights of the different molar mass components [5]. Simple attempts to measure the memory function directly by means of short excitation pulses suffer, however, from poor signal-to-noise ratios due to the low spectral power density of the excitation. Measurements with finite length pulses yield good signal-to-noise ratios, but only the convolution of the memory function with the excitation. Due to 'holes' in the spectrum a simple deconvolution is not possible.

In the following it is shown how pseudostochastic random binary sequences together with fast Fourier transform and correlation techniques can be employed to provide excitations with approximately white power spectra and high spectral power density for the measurement of the linear response function of the concentration mode. Not all random binary sequences, however, fulfil the requirement of a flat power spectrum. Excitations with deconvolutable random binary sequences may also be viewed as spectroscopic experiments

in the frequency domain with frequency multiplexing, which yield the complex diffusion susceptibility, defined as the Fourier transformed of the linear response function.

2 Theory

2.1 TDFRS Signal generation

In the following the concept of TDFRS will be outlined in a compact notation to provide the fundamental equations needed for the main part of this paper. For a more detailed discussion of the phenomenological model and the experimental setup the reader is referred to the literature [1, 2, 3, 5, 6, 7, 8].

For a description of the Ludwig-Soret effect in a binary liquid an extension of Fick's second law of diffusion is employed to calculate the temporal and spatial evolution of the concentration $c(x,t)$, measured in weight fractions, under the boundary conditions imposed by the experiment:

$$\frac{\partial c}{\partial t} = D\Delta c + D_T c(1-c)\Delta T \ . \tag{1}$$

$T(x,t)$ is the time dependent temperature distribution, D the translational and D_T the thermal diffusion coefficient. For TDFRS, $T(x,t)$ is obtained from the heat equation with the energy absorbed from the optical interference grating $I(x,t) = I_0 + I_q \mathrm{e}^{iqx}$ as the source term:

$$\frac{\partial T}{\partial t} = D_{th}\Delta T + \frac{\alpha}{\rho c_p}(I_0 + I_q \mathrm{e}^{iqx}) \tag{2}$$

Because of the underlying symmetry of the holographic experiment, a onedimensional description has been adopted with the x-axis defined by the grating vector $q = 4\pi\lambda^{-1}\sin\theta/2$. θ is the angle between the two writing beams, D_{th} the thermal diffusivity, α the absorption coefficient, ρ the density, and c_p the specific heat at constant pressure. From Eq. 2 the time dependent temperature distribution

$$T(x,t) = T_q(t)\mathrm{e}^{iqx} \tag{3}$$

with

$$T_q(t) = \frac{\alpha}{\rho c_p}\int_{-\infty}^{t} dt' I_q(t')\mathrm{e}^{-(t-t')/\tau_{th}} \tag{4}$$

is obtained, neglecting spatially constant terms. $\tau_{th} = (D_{th}q^2)^{-1}$ is the heat diffusion time constant. Knowing $T(x,t)$ the time dependent concentration distribution is obtained from Eq. 1:

$$c(x,t) = c_0 + c_q(t)\mathrm{e}^{iqx} \tag{5}$$

with

$$c_q(t) = -q^2 D_T c_0(1-c_0) \int_{-\infty}^{t} dt' T_q(t') \mathrm{e}^{-(t-t')/\tau} \ . \tag{6}$$

$\tau = (Dq^2)^{-1}$ is the mass diffusion time constant. Since the concentration changes are generally very subtle, the approximation $c_0 \approx c$ will be used in the following.

Both c and T couple to the refractive index n, resulting in a phase grating

$$n(x,t) - n_0 = n_q(t)\mathrm{e}^{iqx} = [(\frac{\partial n}{\partial T})_{c,p} T_q(t) + (\frac{\partial n}{\partial c})_{T,p} c_q(t)]\mathrm{e}^{iqx} \tag{7}$$

which is read by Bragg diffraction of a readout beam.

The heterodyne diffraction efficiency $\zeta_{het}(t)$, which is proportional to the refractive index modulation depth $n_q(t)$, is obtained after normalization to the signal generated by the temperature grating alone:

$$\zeta_{het}(t) = [\tau_{th} \frac{\alpha}{\rho c_p} I_0]^{-1} \int_{-\infty}^{t} dt' g(t-t') T_q(t') \ . \tag{8}$$

The memory or linear response function $g(t)$ is [1]

$$g(t) = \begin{cases} \delta(t) - (\frac{\partial n}{\partial c})_{p,T} (\frac{\partial n}{\partial T})_{p,c}^{-1} q^2 D_T c(1-c) \mathrm{e}^{-t/\tau} & t \geq 0 \\ 0 & t < 0 \end{cases} \tag{9}$$

Dilute solutions of polydisperse polymers, which cannot be described by a single diffusive mode, are of particular interest. In this case Eq. 9 must be replaced by a sum over all species k present in the sample:

$$g(t) = \sum_k g_k(t) = \delta(t) + \sum_k a_k \mathrm{e}^{-t/\tau_k} \tag{10}$$

$$a_k = -q^2 (\frac{\partial n}{\partial T})_{p,c}^{-1} (\frac{\partial n}{\partial c_k})_{p,T,c_{l \neq k}} \ D_{T,k} c_k \ . \tag{11}$$

Here the dilute solution approximation $c(1-c) \approx c$ has been made.

At least in case of dilute solutions of high polymers there is a time scale separation of more than three decades between the heat and the concentration mode, and for experiments on the time scale of the concentration mode the temperature grating almost instantaneously follows the optical one. Furthermore, $(\partial n/\partial c_k)_{p,T}$ and D_T are approximately independent of molar mass [9], which reduces the molar mass dependence of a_k to the concentration c_k.

Generally, an experiment measures a convolution of the memory function of the concentration mode, $g(t)$, with the time dependent temperature excitation $T_q(t)$. A straight

[1] contrary to $G(t)$ used in previous publications, $g(t)$ has been chosen for a more consistent notation

forward experiment consists of a long excitation pulse of finite length $\tau_p \gg \tau_k$ and constant amplitude. For polydisperse polymer solutions this results in a multiexponential decay function with statistical weights $a_k\tau_k$ for the k-th mode.

Ideally, the memory function $g(t)$, which contains all information that can be learned from a linear experiment, would be measured directly. In the most simple case this is accomplished by shortening the excitation pulse to $\tau_p \ll \tau_k$, where a multiexponential decay function with statistical weights proportional to a_k or, within above approximations, proportional to c_k is obtained [5].

It is of interest to compare heterodyne TDFRS with the electric field autocorrelation function as measured by PCS, the most widely applied technique for the measurement of diffusion coefficients. With a scaling relation $D \propto M^{-b}$, $b \leq 1$, for the molar mass dependence of the diffusion coefficient the statistical weights for the multiexponential decay functions are $c_k M_k^{\alpha}$, where α is characteristic for the experiment [5]. For TDFRS with short pulses $\alpha = 0$, with long excitation pulses $\alpha = b$ is found. The change of the average rate $\langle\Gamma\rangle = \langle\tau^{-1}\rangle$ as a function of exposure time is shown in Fig. 1 for a polydisperse sample. For PCS $\alpha = 1$, resulting in a strong overestimation of the high molar mass components in the PCS autocorrelation function.

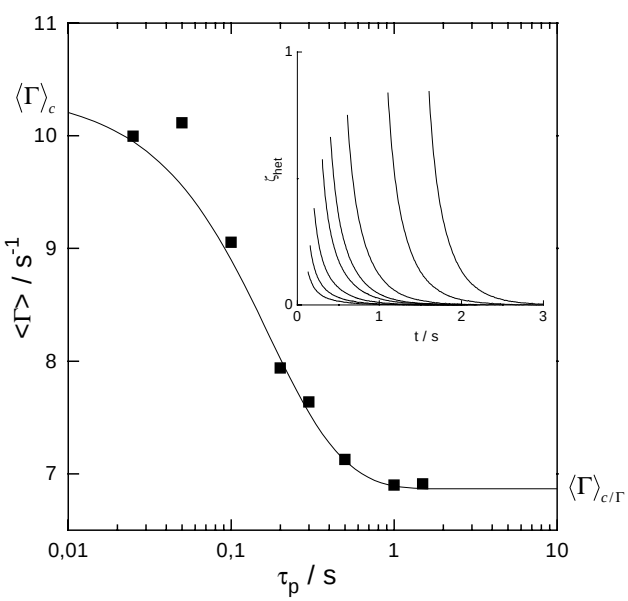

Figure 1: Exposure time dependence of the average rate $\langle\Gamma\rangle$ for a mixture of polystyrene with $M = 48$ and $M = 556$ kg/mol at equal concentration of 0.0029 weight fractions. Exposure ranges from $t = 0$ up to the start of the respective decay curve. The data are taken from reference [5].

2.2 Measurement of the memory function

The problem when measuring $g(t)$ directly by employing short exposure times is obvious from the vanishing signal amplitudes in the insert in Fig. 1, resulting in poor signal-to-noise ratios. The alternative of a straight forward deconvolution of a measurement with a finite pulse length is also not feasible due to holes in the power spectrum of the excitation.

A rather elegant way to measure the response function of a linear system emerged with the cheap availability of fast digital computer hardware in combination with fast Fourier transform and correlation algorithms. The basic idea is to use a deconvolutable excitation with a flat, e.g. white, power spectrum of high spectral power density in combination with tailored deconvolution or correlation techniques. Such excitations can be realized by means of suitable pseudostochastic binary noise sequences. A special variant of such sequences, maximum length binary sequences (MLBS) [10], has successfully been used for Hadamard-NMR-spectroscopy [11].

Fundamental equations: Before turning to the actual experiment some general features of linear systems, as far as they pertain to TDFRS, will briefly be summarized in a problem-independent notation. Later the respective quantities will be mapped to the TDFRS experiment. The convention obeyed is as follows:

Signals are continuous functions in the time domain and denoted in lower case with the argument in parentheses, e.g. $x(t)$. Sampling at constant intervals Δt produces a discrete approximation $x[n]$ to the continuous signal, which is only defined at times $t = n\Delta t,\ n = 0, 1, 2 \ldots$. Square brackets are used for the arguments of discrete functions. The Fourier transform establishes the connection between the time and frequency domain [12]:

$$x(t) = \frac{1}{2\pi} \int_{-\infty}^{\infty} d\omega\ X(\omega)\ \mathrm{e}^{i\omega t} \tag{12}$$

$$X(\omega) = \int_{-\infty}^{\infty} dt\ x(t)\ \mathrm{e}^{-i\omega t} \tag{13}$$

Frequency domain functions are denoted with upper case letters. Of importance for the TDFRS experiment is the discrete Fourier transform of an array of N data points within a period of $N\Delta t$:

$$x[n] = \frac{1}{N} \sum_{k=0}^{N-1} X[k]\ \mathrm{e}^{2\pi i n k/N} \tag{14}$$

$$X[k] = \sum_{n=0}^{N-1} x[n]\ \mathrm{e}^{-2\pi i n k/N} \tag{15}$$

The connection with the frequency scale is given by

$$\omega_k = \frac{2\pi k}{N\Delta t} \ . \tag{16}$$

The response $y(t)$ of a linear system to an excitation $x(t)$ is a convolution of $x(t)$ with the response function $h(t)$:

$$y(t) = x(t) * h(t) \equiv \int_{-\infty}^{t} dt' x(t') h(t - t') \tag{17}$$

The TDFRS experiments discussed are performed with periodic boundary conditions, asking for the discrete periodic convolution

$$y[n] = x[n] * h[n] \equiv \sum_{i=0}^{N-1} x[i] h[(n-i) \mathrm{mod} N] \ . \tag{18}$$

The convolution theorem turns Eqs. 17 and 18 into simple products in frequency space:

$$Y = X \ H \tag{19}$$

The discrete periodic correlation is defined in analogy as

$$y[n] = x[n] \times h[n] \equiv \sum_{i=0}^{N-1} x[i] h[(n+i) \mathrm{mod} N] \ , \tag{20}$$

$$Y = X^* \ H \ . \tag{21}$$

X^* is the complex conjugate of X. No arguments are used in Eqs. 19 and 21 since they apply to both the continuous and discrete case.

From Eqs. 19 and 21 it is immediately evident that h is obtained from the deconvolution

$$H = \frac{Y}{X} = \frac{Y X^*}{|X|^2} \ , \tag{22}$$

followed by the transition to the time domain according to Eq. 12. From the right hand side of Eq. 22 it follows that h may also be determined by cross correlation of the sample response y with the excitation x in case of a white power spectrum with $|X|^2 = 1$.

Definition of the response function: Before Eq. 22 can be applied to the experimental problem the signal flow in the experiment must be considered in detail to identify the proper response function, the corrections that must be applied, and the errors inferred by discrete sampling of the continuous signals. The signal flow is summarized in Fig. 2, and a suitable mapping between the signals in the figure and the actual physical quantities is the following:

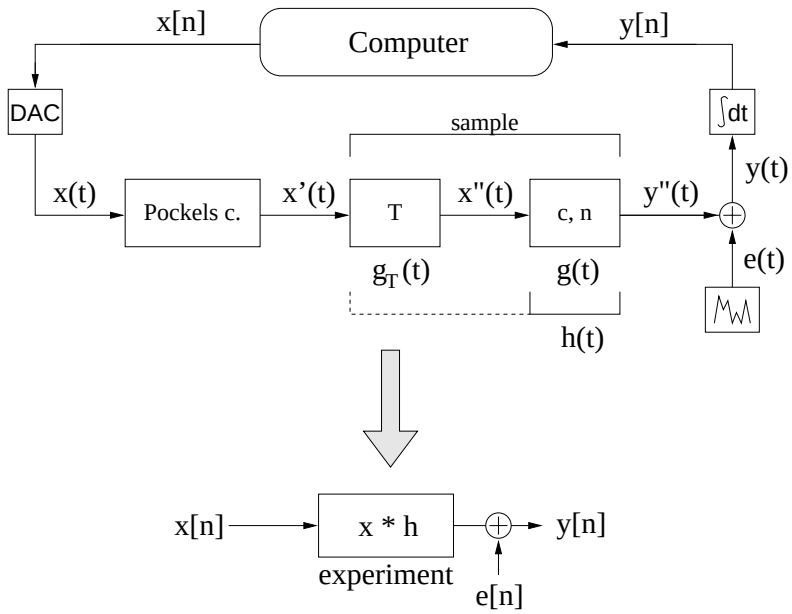

Figure 2: Sketch of the signal generation. See text for details.

A discrete binary sequence $x[n]$ of 1 and -1, defined at times $n\Delta t,\ n = 0, 1 \ldots N-1$, is generated within the computer memory and converted to a continuous binary voltage signal $x(t)$, which drives the high voltage generator for the Pockels cell. The resulting amplitude of the optical interference grating, $x'(t) \equiv I_q(t)/I_0$, excites the sample, which in principle could be described by a single response function $h'(t) = g_T(t) * g(t)$. $h'(t)$ is the convolution of the heat and the concentration mode as indicated by the dashed bracket in Fig. 2.

Due to the time scale separation of 3 to 4 decades between both modes it is, however, more convenient to focus on the response of the concentration mode and convolute the heat mode $g_T(t) = \tau_{th}^{-1} \exp(-t/\tau_{th})$ into the effective excitation, hence

$$x''(t) = T_q(t)[\frac{\alpha}{\rho c_p} I_0 \tau_{th}]^{-1} \ . \tag{23}$$

$T_q(t)$ is given in Eqs. 3 and 4.

Now, the effective linear response function $h(t)$ can be identified with $g(t)$ as defined in Eqs. 9 and 10: $h(t) \equiv g(t)$. It contains both the response of the concentration mode and the infinitely fast translation of the concentration and the driving temperature grating into the measurable heterodyne diffraction efficiency $y''(t) \equiv \zeta_{het}(t)$. The instantaneous contribution of the temperature grating to the diffraction efficiency is expressed by the δ-function in $g(t)$. After the sample an unavoidable noise term $e(t)$ is added. The continuous signal $y(t)$ is sampled by integrating with an ideal detector over time intervals Δt to obtain the time discrete sequence $y[n]$ for processing in the computer.

There are several reasons why we focus on $g(t)$ and not the entire response function of the sample, $g_T(t) * g(t)$. The first one is trivial, since our main interest is not heat transport but mass and thermal diffusion in polymeric systems. Furthermore, experience shows that in a typical experiment with long step-like excitations the measured amplitudes from both modes are approximately equal. Since these saturation amplitudes are proportional to the respective time constants τ_{th} and τ, it is straight forward to show that this translates into a difficult to handle amplitude ratio of up to 10^4 between the fast heat and the slow concentration mode in the total response function $g_T(t) * g(t)$. By convoluting $g_T(t)$ into the excitation and employing sample times $\tau_{th} \ll \Delta t \ll \tau$ the disparity between both signal amplitudes reduces to a much more convenient $\mathrm{O}(\tau/\Delta t)$.

In summary, the TDFRS experiment converts an ideal time discrete excitation $x[n]$ into a time discrete signal $y[n]$, involving both linear and nonlinear components like the sample itself or the Pockels cell. The task is to extract the response $h(t) \equiv g(t)$ from $y[n]$ when $x[n]$ is known. This idealized view of the experiment is shown in the lower part of Fig. 2. All the missing components from the upper part of Fig. 2 are treated as perturbations, which can be accounted for in a well conducted experiment.

2.3 Selection of the excitation pattern

So far not much has been said about the excitation sequence $x[n]$, except that the considerations will be restricted to binary sequences of amplitude +1 and -1, corresponding to 180° phase jumps of the holographic intensity grating at maximum modulation depth. Such binary sequences combine the advantage of high spectral power density for linear heterodyne detection with easy experimental handling.

Noise amplification: The total power P in the excitation is obtained from Parseval's theorem:

$$P = \sum_{k=0}^{N-1} |X[k]|^2 = N \sum_{n=0}^{N-1} x[n]^2 \tag{24}$$

Since the power at zero frequency, $|X[0]|^2$, merely adds a constant background without much information content, the requirement for maximum excitation power P_+ at positive frequencies is

$$P_+ = \sum_{k=1}^{N-1} |X[k]|^2 = N \sum_{n=0}^{N-1} x[n]^2 - (\sum_{n=0}^{N-1} x[n])^2 = N^2(\langle x^2 \rangle - \langle x \rangle^2) \ . \tag{25}$$

P_+ reaches maximum for $\langle x \rangle = 0$. Hence, an excitation sequence should contain at least approximately the same number of +1 and -1.

Further constraints are imposed by the unavoidable noise term $e[n]$, which adds to the signal:

$$Y = XH + E \ . \tag{26}$$

The arguments are omitted and the frequency domain notation has been chosen for simplicity. After deconvolution the experimentally determined memory function contains the true memory function plus an error term:

$$\frac{YX^*}{|X|^2} = H + E\ \frac{X^*}{|X|^2} \tag{27}$$

From Eq. 27 the amplification U_k of the spectral power density of the noise is

$$U_k = |\frac{X^*[k]}{|X[k]|^2}|^2 = |X[k]|^{-2} \ , \tag{28}$$

and the integral noise amplification

$$U = \sum_{k=0}^{N-1} |X[k]|^{-2} \ . \tag{29}$$

U is minimized for a constant white power spectrum with $|X[k]|^2 = N$ according to Eq. 24, yielding $U = 1$. All deviations from the constant power spectrum increase the integral noise amplification U. They may, however, be employed for noise suppression at selected frequencies.

Arbitrary random binary sequences generally have a globally flat power spectrum but a high noise amplification due to a locally rugged structure of the spectral power density with large values of U_k. Efficient excitation sequences can be generated from random binary sequences by successive optimization. This problem is equivalent to the one of minimizing the energy of an Ising spin system, where the spins are represented by the excitation pulses (+1 or -1) and the energy U is defined in Eq. 29. With simple one-spin-flip optimization, where subsequently all spins are tested and flipped only if the energy is reduced, $U \approx 1.15$ is easily achieved. More sophisticated techniques, like simulated annealing, give only slight improvements [13]. For practical purposes such optimized sequences are almost ideal. As an example, optimization reduces the noise amplification of a particular but arbitrarily chosen random binary sequence of length $N = 2^{12}$ from $U = 17.3$ to $U = 1.18$, which is almost identical to the theoretical limit $U = 1$ for all practical purposes.

Another class of suitable excitations with a perfectly white power spectrum are maximum length binary sequences (MLBS) of length $N = 2^L - 1$, L being a positive integer [10]. MLBS have been employed in Hadamard NMR spectroscopy [11], and the deconvolution

according to Eq. 22 is efficiently computed by means of a fast Hadamard transform. The performance of MLBS in TDFRS is approximately the same as the one of optimized random sequences. Some peculiarities have been found for MLBS with respect to systematic distortions introduced by the Pockels cell [14]. The computational effort for MLBS of length $N = 2^L - 1$ and sequences of length 2^L is comparable when fast finite Fourier transform algorithms are used.

2.4 Corrections and limitations

The parts of the experiment that have been omitted when using the simplified description according to Fig. 2 necessitate some corrections and impose limitation that will briefly be discussed in the following.

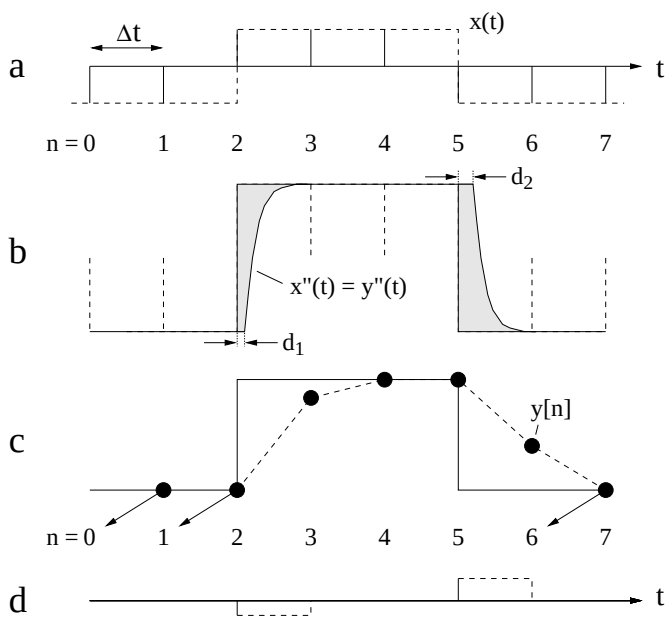

Figure 3: Details of the measurement: ideal excitation (a), amplitude of the temperature grating and of the heterodyne signal for $c = 0$ (b), effect of sampling for $y(t) \rightarrow y[n]$ (c), and fictive correction to the ideal excitation (d).

Fig. 3 gives a closer look of the measurement process for a hypothetic sample, for simplicity without dissolved polymer. The binary sequence $x[n] = [-1, -1, 1, 1, 1, -1, -1, -1 \ldots]$ is defined at times $t = n\Delta t$ and converted to the continuous excitation $x(t)$, which keeps the value $x[n]$ from $t = n\Delta t$ until $t = (n + 1)\Delta t$ as indicated by the dashed line in Fig. 3a.

The temperature grating $x''(t)$ (Fig. 3b) does not follow $x(t)$ instantaneously because of its finite time constant $\tau_{th} \ll \Delta t$ and because there is a delay of several μs caused by the

high voltage driver for the Pockels cell, which is asymmetric with respect to the switching direction (d_1 and d_2). As a consequence, everytime the excitation changes its sign there is some intensity missing in the excitation as shown by the shaded areas.

Sampling is done by integration from $t = n\Delta t$ to $t = (n+1)\Delta t$, and the result is stored in $y[n]$ (Fig. 3c). To interprete the data as the average over the respective interval the time scale for $g(t)$ is shifted by $\Delta t/2$ towards higher values.

In the expample, the effect of the missing area manifests itself for $y[2]$ and $y[5]$. The finite temperature response and the delay can approximately be accounted for by adding a fictive excitation x_f proportional to the derivative of the ideal excitation to $x[n]$. The asymmetry $d_1 - d_2$ is incorporated in an analogous way, hence

$$x_f[n] = a(x[n] - x[n-1]) + b(x[n] - x[n-1])(1 - x[n-1]) \ . \tag{30}$$

$x_f[n]$ and $x_f(t)$ are shown in Fig. 3d. a and b are constants and can be determined from separate measurements of the Pockels cell response and τ_{th}. In the language of digital signal analysis a is due to aliasing of signal intensity with frequencies above the Nyquist frequency $\omega_{Ny} = \pi/\Delta t$, which are folded back into the frequency interval $-\omega_{Ny} < \omega_k < \omega_{Ny}$. $a = 0$ may be used for simplicity, in which case the thermal amplitude is spread over a few data points instead of being confined to the first one according to the δ-function in Eq. 9. The area is, however, preserved. To avoid signal distortion due to aliasing of the interesting mass diffusion part of the spectrum the sampling time should, as a rule of thumb, fulfil $\Delta t \leq \tau/10$ for the fastest concentration mode. On the other hand, Δt should not be shorter than necessary, since the signal to noise ratio can shown to be proportional to $N^{1/2}\Delta t$. This is an improvement by a factor $N^{1/2}$ over single pulse δ-excitations with pulse length Δt.

3 Experiment

The setup is almost identical to the one used for previous experiments. An argon ion laser (488 nm) is used for writing and a helium-neon laser (633 nm) for reading. Switching of the grating is accomplished by 180° phase shifts by means of a Pockels cell in one of the writing beams such that +1 in the excitation sequence corresponds to a phase of 0° and -1 to 180°. A reference wave is provided by scratches or dust on the sample, serving as local oscillator. The phase between the reference and the signal beams is adjusted by means of a piezo mirror. A PMT in photon counting mode is used for detection. A custom made plug-in card in a PC is used for photon counting and also controls the timing

and synchronization between the excitation sequence and the measured PMT signal. The measurements are done in bursts of several repetitions of the excitation sequence $x[n]$ where the first N data points are discarded. Since the system memory is much shorter than $N\Delta t$, truly periodic boundary conditions are achieved.

All experiments have been conducted in heterodyne mode, and the TDFRS setup and the separation of homodyne and heterodyne signal components has been described in detail in [7]. The solutions are slightly colored with quinizarin to adjust the optical density to 0.02 at the writing wavelength. The pathlength of the optical cell is 200 μm. All measurements have been performed at room temperature.

4 Results

Fig. 4 shows an experiment on almost monodisperse polystyrene (PS, $M \approx 250000$ g/mol) in toluene at a concentration of $c = 0.0205$. The scattering vector $q = 9213$ cm^{-1} is well within the hydrodynamic limit $qR_g \ll 1$, where pure center of mass diffusion is observed. R_g is the radius of gyration of the polymer. The upper part of the insert is a section of the pulse train of the optimized random binary sequence of length $N = 2^{11}$ used for excitation with a time resolution of $\Delta t = 140\mu s$. The lower part of the insert represents the normalized heterodyne diffraction efficiency. The main portion of Fig. 4 shows the concentration part of the memory function $g(t)$ as obtained by deconvolution. For the diffusion time constant $\tau = 13900$ μs, corresponding to $D = 5.5 \times 10^{-7}$ cm^{2}s^{-1} has been found.

The amplitude of the temperature signal in $g(t)$ is normalized to unity and not plotted in Fig. 4. Due to aliasing it is spread over the first three data points.

A comparison between TDFRS and PCS for a solution of a bimodal molar mass distribution is shown in Fig. 5. The sample is a mixture of two PS with 895 and 250000 g/mol and a dispersity of $M_w/M_n \approx 1.03$ in toluene at concentrations of 0.0166 and 0.00228, respectively.

The heterodyne decay functions for a TDFRS experiment with pseudostochastic noise excitation and for a TDFRS experiment with step-excitation are plotted together with the electric field autocorrelation function from PCS in the upper half of Fig. 5. The PCS experiment has been performed at an angle of 90° and a wavelength of 647 nm and the time scale has been shifted according to $\tau \propto q^{-2}$. The TDFRS parameters are $\Delta t = 140\mu s$ and $N = 2047$. Blocks of 16 repetitions of the excitation sequence have been accumulated

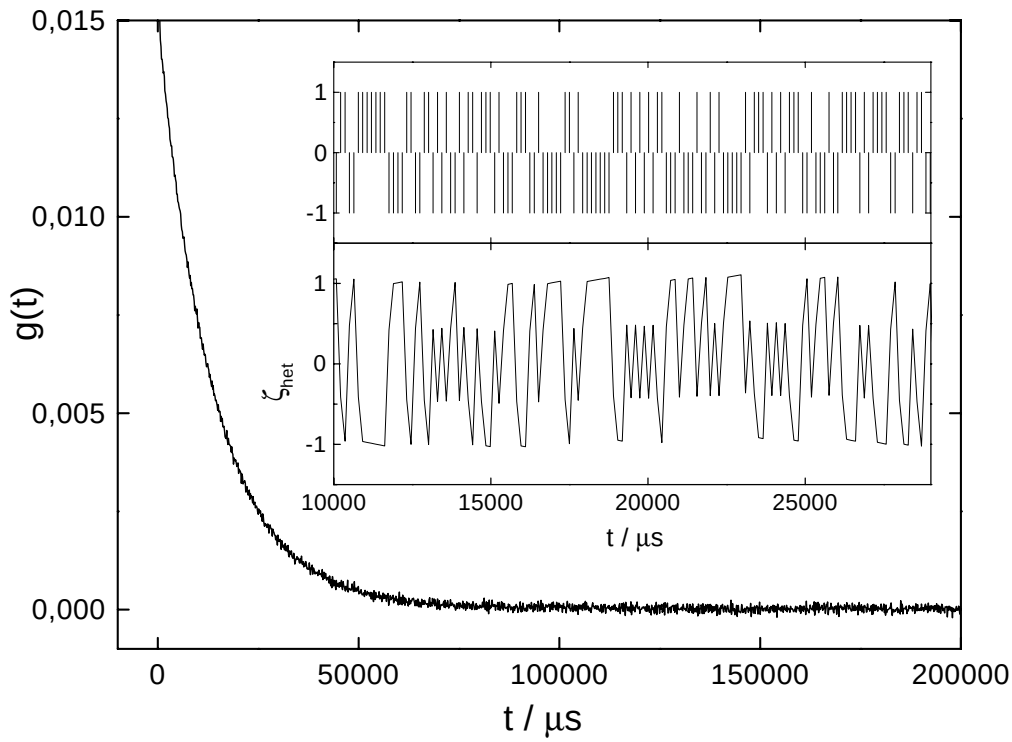

Figure 4: Memory function $g(t)$ as obtained from optimized random binary sequence with $N = 2048$. The insert shows a section of the excitation sequence and the corresponding measured heterodyne sample response.

between phase stabilizations for heterodyne detection and the signal has been averaged over 488 such blocks. The same overall time has been used for all three experiments. The solid lines are biexponential least square fits. Both modes are clearly visible in the TDFRS measurements, whereas the PCS correlation function is completely dominated by the slow mode of the high molar mass, despite the sevenfold higher concentration of the low molar mass component. In a PCS experiment on the low molar mass component alone no diffusion process that exceeded the baseline noise could be observed.

The lower half of Fig. 5 shows the rate distributions for TDFRS with pseudostochastic noise excitation and for PCS as obtained from an inverse Laplace transform using CONTIN [15]. Again, both components are clearly resolved by TDFRS. The PCS rate distribution shows only a large peak for the slow mode. The tiny peak at $\tau^{-1} \approx 1.7 \times 10^{-3}$ s^{-1} is probably an artifact, since its rate is too high when compared with the well resolved TDFRS. The amplitude ratio obtained from the rate distribution for $g(t)$ is 6.8, which is reasonably close to the one expected from the polymer concentrations and the refractive index increments: $[c_1(\partial n/\partial c_1)_{p,T}][c_2(\partial n/\partial c_2)_{p,T}]^{-1} = 5.9$. For the refractive index increments the zero concentration values (0.0736 and 0.0907) of the respective molar mass polymers (895 and 250000 g/mol) have been determined using an interferometric refrac-

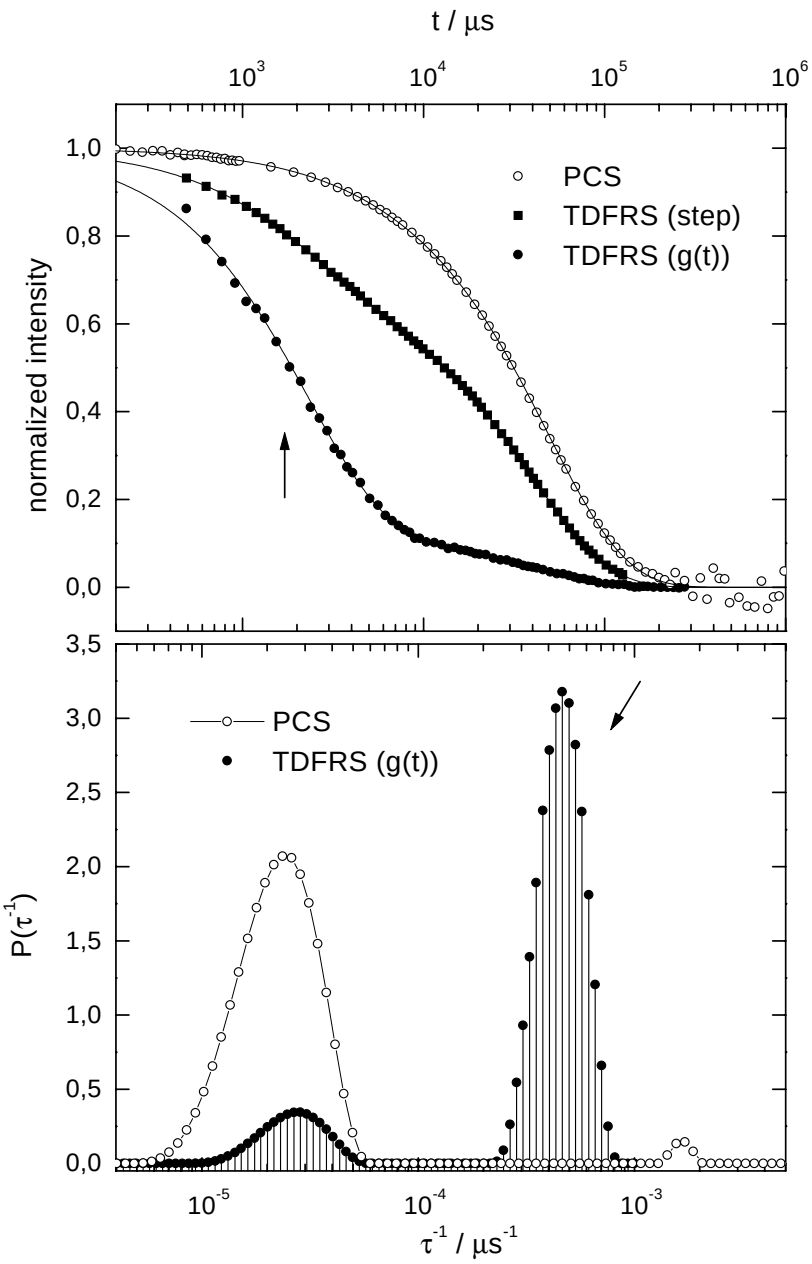

Figure 5: Comparative measurement of bimodal PS in toluene with PCS and TDFRS with optimized random binary sequence and with step excitation; decay functions (upper) and rate distributions (lower). The fast mode of the light component (895 g/mol) is marked by arrows.

tometer [16]. The molar mass dependence of $(\partial n/\partial c)_{p,T}$ is due to end group effects of the short chains. From $g(t)$ the thermal diffusion coefficient is calculated according to Eqs. 10 and 11 as $D_T = 1.12 \times 10^{-7}$ cm^2(sK)$^{-1}$, which is in excellent agreement with results found previously in the same laboratory [6].

Fig. 6 shows the diffusion susceptibility, which has directly been obtained from the

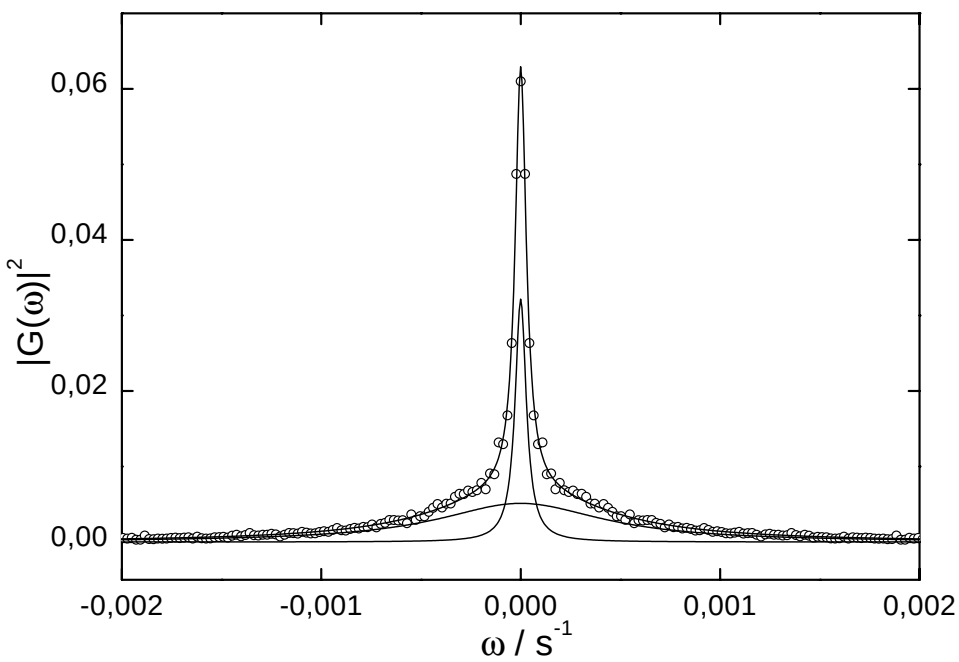

Figure 6: Diffusion susceptibility $|G(\omega)|^2$ as obtained from the measurement of $g(t)$ in Fig. 5 with least square fit of two Lorentzians, which are also plotted separately.

measurement as the Fourier transformed of $g(t)$ from Fig. 5, plotted as $|G(\omega)|^2$. The solid lines are least square fits of the two Lorentzians corresponding to the two approximately exponential modes in $g(t)$:

$$|G(\omega)|^2 = |\frac{a_1\tau_1}{1+\mathrm{i}\omega\tau_1} + \frac{a_2\tau_2}{1+\mathrm{i}\omega\tau_2}|^2 \tag{31}$$

5 Summary and conclusion

Signal generation in heterodyne TDFRS can be formulated in the language of linear response theory. For the measurement of diffusion processes it is advantageous to focus on the concentration modes and to lump the temperature response into the excitation. Especially for dilute polymer solutions the response function $g(t)$ of the concentration modes shows interesting properties like concentration proportional amplitudes of the individual molar mass components. While, due to a poor signal-to-noise ratio, a straight forward measurement of $g(t)$ as response to a δ-excitation is not feasible, pseudostochastic random binary sequences provide an elegant and efficient access to $g(t)$.

For a correct interpretation of the experiment various corrections and and limitations must be considered to avoid problems from e.g. aliasing. Perfectly white power spectra

are realized with MLBS. Optimized random binary sequences offer almost the same noise amplification and the additional opportunity of coloring the excitation spectrum by shifting energy into interesting frequency ranges. A detailed discussion of colored spectra is, however, beyond the scope of this paper.

Besides the direct measurement of the linear response function, pseudostochastic random binary sequences provide additional advantages such as time scale delocalization and frequency multiplexing. As a consequence of time scale delocalization a singular perturbation from e.g. dust particles does not deform the decay function locally but is spread over the entire time axis as random noise. Frequency multiplexing drastically reduces the stability requirement for experiments in the frequency domain in order to obtain the diffusion susceptibility $G(\omega)$. If all frequencies were measured subsequently, stability over the whole duration of the experiment would be required, whereas frequency multiplexing reduces the stability requirement to several excitation periods $N\Delta t$.

From a well conducted experiment precise values for the transport coefficients are obtained, as has been demonstrated for a bimodal PS mixture. For this polydisperse sample both components are resolved and the low molar mass component has been recovered with a large concentration proportional amplitude, whereas the PCS correlation function is entirely dominated by the heavy component.

Acknowledgements

The authors thank C. Rosenauer for the PCS measurements and B. Müller for the measurement of the refractive index increments.

References

[1] K. Thyagarajan and P. Lallemand. *Opt. Commun.*, 26:54 (1978).

[2] F. Bloisi, L. Vicari, P. Cavaliere, S. Martellucci, J. Quartieri, P. Mormile, and G. Pierattini. *Appl. Phys.*, B44:103 (1987).

[3] W. Köhler. *J. Chem. Phys.*, 98:660 (1993).

[4] F. Bloisi. *Opt. Commun.*, 68:87 (1988).

[5] P. Rossmanith and W. Köhler. *Macromolecules*, 29:3203 (1996).

[6] W. Köhler, C. Rosenauer, and P. Rossmanith. *Int. J. Thermophys.*, 16:11 (1995).

[7] W. Köhler and P. Rossmanith. *J. Phys. Chem.*, 99:5838 (1995).

[8] W. Köhler and B. Müller. *J. Chem. Phys.*, 103:4367 (1995).

[9] M. E. Schimpf and J. C. Giddings. *J. Polym. Sci., Polym. Phys.*, B27:1317 (1989).

[10] D. Ziessow. On-line Rechner in der Chemie. (de Gruyter, Berlin, 1973).

[11] D. Ziessow and B. Blümich. *Ber. Bunsenges. Phys. Chem.*, 78:1168 (1974).

[12] S. D. Stearns. Digitale Verarbeitung analoger Signale. (Oldenburg, München, 1987).

[13] W. Köhler and R. Schäfer. *to be published*, 1997.

[14] R. Schäfer. PhD thesis, Johannes-Gutenberg Universität, Mainz, 1997.

[15] S. W. Provencher. *Computer Phys. Commun.*, 27:229 (1982).

[16] A. Becker, W. Köhler, and B. Müller. *Ber. Bunsenges. Phys. Chem.*, 99:600 (1995).